Analytical Biochemistry 379 (2008) 60–65

Contents lists available at ScienceDirect

Analytical Biochemistry

journal homepage: www.elsevier.com/locate/yabio

A colorimetric assay for steady-state analyses of iodo- and bromoperoxidase activities

Elodie Verhaeghe [a], David Buisson [a], Elisabeth Zekri [a], Catherine Leblanc [b], Philippe Potin [b], Yves Ambroise [a,*]

[a] CEA, iBiTecS, Service de Chimie Bioorganique et de Marquage, Gif sur Yvette F-91191, France
[b] CNRS, Université Pierre et Marie Curie, Station Biologique de Roscoff, Dispersal and Adaptation in Marine Species, UMR-7139, Roscoff F-29682, France

ARTICLE INFO

Article history:
Received 31 January 2008
Available online 27 April 2008

Keywords:
Iodoperoxidase
Bromoperoxidase
Thymol blue
Vanadium

ABSTRACT

The standard assay for iodoperoxidase activity is based on the spectrophotometric detection of triiodide formed during the enzymatic reaction. However, chemical instability of I_3^- has limited the method to high iodide concentrations and acidic conditions. Here we describe a simple spectrophotometric assay for the determination of iodoperoxidase activities of vanadium haloperoxidases based on the halogenation of thymol blue. The relation between color and chemical entities produced by the vHPO/H_2O_2/I^- catalytic system was characterized. The method was extended to bromine and, for the first time, allowed measurement of both iodo- and bromoperoxidase activities using the same assay. The kinetic parameters (K_m and k_{cat}) of bromide and iodide for vanadium bromoperoxidase from *Ascophyllum nodosum* were determined at pH 8.0 from steady-state kinetic analyses. The results are concordant with an ordered two-substrate mechanism. It is proposed that halide selectivity is guided by the chemical reactivity of peroxovanadium intermediate rather than substrate binding. This method is superior to the standard I_3^- assay, and we believe that it will find applications for the characterization of other vanadium as well as heme haloperoxidases.

Halogenation reactions in biological systems are catalyzed mainly by enzymes and are essential to the biosynthesis of many natural products [1]. Unfortunately, little is known about the mechanisms of these enzymatic halogenations. Currently, two distinct classes of halogenating enzymes have been categorized based on the nature of their cosubstrate. The flavin-dependent and nonheme, Fe^{2+}-dependent enzymes require O_2 as an electron acceptor and have been termed O_2-dependent halogenases. In contrast, the Feheme- and vanadium-dependent enzymes use H_2O_2 as a cosubstrate and are termed haloperoxidases [2].

Haloperoxidases catalyze the two-electron oxidation of halides in the presence of hydrogen peroxide. They are named according to the most electronegative halide that they can oxidize. Chloroperoxidases (CPOs)[1] catalyze the oxidation of chloride, bromide, and iodide; bromoperoxidases (BPOs) catalyze the oxidation of bromide and iodide, and iodoperoxidases (IPOs) are specific for iodide. Since the first discovery of a fungal CPO 40 years ago [3], heme-containing haloperoxidases have been characterized in animals and halide metabolism was shown to be essential in the physiology of vertebrates. Thyroid peroxidase (IPO-like) plays a key role in the synthesis of thyroid hormones T3 and T4, which are essential for the development and maturation of many organs, especially of the nervous system [4]. Myeloperoxidase (CPO-like) in neutrophils, eosinophil peroxidase (BPO-like enzyme) in phagocytes, and lactoperoxidase (BPO-like) found in human exocrine secretions are involved in host defense and antimicrobial effects [5]. In marine algae, another class of haloperoxidases, the vanadium-dependent haloperoxidase (vHPO), is likely to play a key role in the production of volatile halocarbons and defense mechanisms. On a larger scale, these halogenated compounds, especially the iodinated ones and molecular iodine, are believed to have a significant impact on atmospheric chemistry [6]. The physiological and environmental importance of halogenation processes, as well as the growing interest of organohalogens as potential pharmaceutical drugs, has elicited a large number of biochemical and chemical studies [2,7].

The halogenation mechanism of both Feheme- and vanadium-dependent haloperoxidases is still highly debated for active site halogenation versus diffusible species-mediated halogenation [8]. Steady-state kinetic analyses of vBPO from a marine brown alga, *Ascophyllum nodosum,* have suggested an ordered bi–bi ping-pong mechanism [9]. It is also well established that during the catalytic cycle of vanadium-containing haloperoxidases, a peroxovanadium intermediate is formed [10]. However, the molecular bases of ha-

* Corresponding author. Fax: +33 16908 7991.
E-mail address: yves.ambroise@cea.fr (Y. Ambroise).

[1] *Abbreviations used:* CPO, chloroperoxidase; BPO, bromoperoxidase; IPO, iodoperoxidase; vHPO, vanadium-dependent haloperoxidase; MCD, monochlorodimedone; I_3^-, triiodide; TB, thymol blue (thymolsulfonphthalein); PEG 1550, polyethylene glycol; DMSO, dimethyl sulfoxide; TBI_2, diiodothymolsulfonphthalein; $TBBr_2$, dibromothymolsulfonphthalein; ESI–TOF, electrospray ionization time-of-flight; HPLC–MS, high-performance liquid chromatography–mass spectrometry; HRMS, high-resolution mass spectrometry.

0003-2697/$ - see front matter © 2008 Elsevier Inc. All rights reserved.
doi:10.1016/j.ab.2008.04.041

lide selectivity between the different haloperoxidases have not yet been elucidated.

The classic method for determining CPO and BPO activities is based on the halogenation of monochlorodimedone (MCD) by released oxidized chlorine or bromine species [3]. Because the optical absorptions of MCD (ε^{290} = 20,000 M^{-1} cm^{-1}) and halo-MCD (ε^{290} = 100 M^{-1} cm^{-1}) are clearly distinct from each other, this reaction has provided a simple assay that has been used to investigate the enzyme kinetic mechanism of vHPO [9,11]. Unfortunately, this assay cannot be applied to the determination of iodoperoxidase activity because MCD is not reactive toward iodination. Phenol red was also reported as a spectrophotometric probe for the detection of vHPO-catalyzed brominating and chlorinating activities [12,13]. However, the halogenation of phenol red is slow and not stoichiometric. For these reasons, this method was used only for qualitative purposes. The measurement of iodoperoxidase activities is based on the spectrophotometric detection of triiodide (I_3^-) at 350 nm [14]. This method has led to the biochemical characterization of specific vIPOs in brown algae of the Laminariaceae family [15,16]. However, the complex nature of iodine chemistry in solution has restricted this assay to a narrow range of experimental conditions (acidic pH, high iodide concentrations) to ensure I_3^- formation and stability.

The availability of an enzymatic test capable of measuring both iodo- and bromoperoxidase activities is essential to investigate the relationships among amino acid compositions, protein structure, and biochemical properties. In this context, we developed a single assay for the measurement of both activities. The method is based on the reactivity of thymolsulfonphthalein (thymol blue [TB]) toward oxidized halogen species. The vHPO-catalyzed halogenation of the sulfonphthalein dye produced stable molecules with distinct spectral properties. We established the correlation between optical modifications in the reaction media and the molecular entities formed during the enzymatic reaction. This assay was applied to the determination of K_m and k_{cat} of iodide and bromide for vanadium bromoperoxidase from *A. nodosum.*

Materials and methods

Purification of vanadium bromoperoxidase from A. nodosum

For extraction and purification of vBPO from *A. nodosum,* we used the aqueous salt/polymer two-phase protocol developed by Vilter [17]. Briefly, 30 g of *A. nodosum* thalli, collected from the shore in the vicinity of Roscoff, Brittany, France, was powdered in liquid nitrogen and extracted in a two-phase solution (1 L) that contained 17.5% (w/v) K_2HPO_4 and 17.5% (w/v) polyethylene glycol (PEG 1550). The two phases were separated by centrifugation at 5000*g* for 15 min, and then 6% (w/v) $MgSO_4$ was added to generate a second phase system. Then 10% (w/v) PEG 1550 was added to remove phenols and chlorophylls from the bottom phase. A third system was generated for desalting by the addition of an equal volume of a solution containing 20% (w/v) PEG 1550 and 60% (w/v) $(NH_4)_2SO_4$. Three volumes of acetone were added to the upper layer, and after 1 h at 20 °C the protein extract was pelleted by centrifugation at 10,000 *g* for 30 min. To reactivate the enzyme, the pellet was dissolved and dialyzed overnight against 2 mM $NaVO_3$ in 50 mM Tris–HCl (pH 9.0). The extract was then loaded on a phenyl-Sepharose CL4B hydrophobic interaction column equilibrated with 30% $(NH_4)_2SO_4$ and 50 mM Tris–HCl (pH 9.0). Proteins were eluted with a decreasing linear gradient down to salt-free Tris–HCl buffer. The vBPO-active fractions were pooled and dialyzed against 50 mM Tris–HCl buffer (pH 9.0). Protein concentration was determined by using a Bradford commercial assay (Bio-Rad) and was checked by denaturing electrophoresis. The same enzyme batch (8 mg/ml) was used for all of the enzymatic assays.

Measurement of I_3^- degradation as a function of pH

The experiments were performed in triplicate at 20 ± 1 °C. Fifteen buffered acetate/phosphate/borate solutions (30 mM) were prepared and adjusted to pH 2.0, 3.0, 4.0, 4.5, 5.0, 5.5, 6.0, 6.5, 7.0, 7.5, 8.0, 9.0, 10.0, 11.0, and 12.0. The buffered solutions were distributed (70 μl) into a clear flat-bottomed, 96-well polystyrene microplate (Costar 9017, Corning Life Sciences). Then 10 μl of I^- (10 mM final), 10 μl of H_2O_2 (2 mM final), and 10 μl of I_2 (0.5 mM final) were successively added to each well. For solubility purposes, I_2 was dissolved in H_2O/MeOH (50:50) in the stock solution (5 mM). The absorbance at 350 nm was immediately recorded on a SpectraMax Plus 384 (Molecular Devices) for 20 min. For each pH, A_{350} values were averaged and converted into I_3^- concentrations using the following parameters: ε = 25 mM^{-1} cm^{-1} and path length = 0.145 cm (for 100 μl in the well, according to the manufacturer). Initial velocities (0–2 min) were calculated by linear regression and were expressed as millimolars of I_3^- degradation per minute (mM min^{-1}). For pH > 8.0, the I_3^- degradation rates were too fast to be measured.

Haloperoxidase activity measurement

All reactions were performed in quadruplicate at 20 ± 1 °C in a clear flat-bottomed, 96-well polystyrene microplate (Costar 9017). The stock solution of TB (1 mM) was prepared in H_2O/dimethyl sulfoxide (DMSO) (4:1), and the final DMSO content never exceeded 2%. The assays were carried out as follows. To the reaction mixture (180 μl), consisting of phosphate buffer (100 mM, pH 8.0), TB (100 μM), NaI (62.5 μM–4 mM) or NaBr (3.125–200 mM), and vBPO (0.05–4.0 μg ml^{-1}), was added 20 μl of H_2O_2 (0.2, 0.35, 0.7, or 1.0 mM final). The absorbance at 620 nm of the resulting mixture (200 μl) was immediately recorded on a SpectraMax Plus 384 for 20 min. The A_{620} values were converted to millimolars of diiodothymolsulfonphthalein (TBI_2) using $[C] = A_{620}/(40.3\ mM^{-1}\ cm^{-1} \times 0.29\ cm)$ and of dibromothymolsulfonphthalein ($TBBr_2$) using $[C] = A_{620}/(37.2\ mM^{-1}\ cm^{-1} \times 0.29\ cm)$. For the determination of kinetic parameters, the experimental initial velocities (0–60 s), expressed in millimolars of X^- converted per minute, were averaged and fitted to the Michaelis–Menten equation using a nonlinear regression program developed in Visual Basic for Excel.

HPLC–MS analysis

HPLC–MS analysis was performed on a system equipped with a binary gradient solvent delivery system (LC-10AT VP, Shimadzu), a system controller (SCL-10 AVP, Shimadzu), and a UV–visible detector (SPD-10A VP, Shimadzu). During the time course of the vBPO-catalyzed reaction, 20 μl (2 nmol of dye) was injected on a 250 × 4.6-mm, 5-μm HyPURITY C18 (Thermo Electron). Samples were eluted isocratically with acetonitrile/water/formic acid (45:55:0.1) at a flow rate of 0.8 ml/min and were detected at 220 nm. TB, $TBBr_2$, and TBI_2 eluted at 8.6, 29.7, and 42.3 min, respectively. The mass spectra were acquired using a electrospray ionization time-of-flight (ESI–TOF) spectrometer (Mariner, Perspective Biosystems). The instrument was operated in the positive mode using a spray voltage of 4.5 kV, a cone voltage of 180 kV, and a source temperature of 180 °C. The scan range was m/z 70 to 1500, and the dwell time was 3 s.

Isolation of TBI_2 and $TBBr_2$

For TBI_2, a mixture of TB (18.6 mg), NaI (1.5 mM), vBPO (50 μg), and H_2O_2 (0.7 mM) in 200 ml phosphate buffer (100 mM, pH 7.2) and 2% DMSO was stirred at 20 °C for 90 min. The reaction mixture

was acidified to pH 1.0 to 2.0 using 2 N HCl (10 ml) and was extracted with dichloromethane (3 × 100 ml). The organic phases were pooled, treated with Na_2SO_4, filtered, and evaporated to dryness to afford pure TBI_2 (26 mg, 90% yield) as a deep pink solid. TBI_2 was further analyzed by high-performance liquid chromatography–mass spectrometry (HPLC–MS, > 99% purity) and high-resolution mass spectrometry (HRMS). For $TBBr_2$, a mixture of TB (9.3 mg), NaBr (10 mM), vBPO (14 μg), and H_2O_2 (0.08 mM) in 200 ml of phosphate buffer (100 mM, pH 7.8) and 2% DMSO was stirred at 20 °C for 3 h. The reaction mixture was acidified to pH 1.0 to 2.0 using 2 N HCl (10 ml) and was extracted with dichloromethane (3 × 100 ml). The organic phases were pooled, treated with Na_2SO_4, filtered, and evaporated to afford 10.7 mg of crude solid. This solid was applied to a preparative thin-layer chromatography plate (SiO_2) and eluted five consecutive times (AcOEt/EtOH, 8.0:1.5). $TBBr_2$ was extracted from the silica using dichloromethane/EtOH (5:2, 2 × 5 ml). The resulting suspension was filtered and evaporated to dryness to afford pure $TBBr_2$ (3.61 mg, 28% yield) as a deep orange solid. $TBBr_2$ was further analyzed by HPLC–MS (> 99% purity) and HRMS.

pK_a determination of TBI_2, $TBBr_2$, and TB

Fifteen buffered phosphate/borate solutions (100 mM) were prepared and adjusted to pH 6.0, 6.3, 6.6, 6.9, 7.2, 7.5, 7.8, 8.1, 8.4, 8.7, 9.0, 9.3, 9.6, 9.9, and 10.2. To each solution was added the sulfonphthalein dye at a final concentration of 100 μM. The absorbance at 620 nm of each solution was recorded at 20 °C using a SpectraMax Plus 384 microplate reader. The A_{620} versus pH was fitted to the following four-parameter sigmoidal equation:

$$A_{620} = A_{620}(\min) + [A_{620}(\max) - A_{620}(\min)]/[1 + 10^{(pK_a - pH)}]$$

where $A_{620}(\min)$ is the absorbance at 620 nm when 100% of the indicator is protonated (i.e., pH ≪ pK_a) and $A_{620}(\max)$ is the absorbance at 620 nm when 100% of the indicator is deprotonated (i.e., pH ≫ pK_a). The pK_a values were determined by nonlinear regression analysis using an "in-house" application developed in Visual Basic for Excel.

Results and discussion

Limitations of the triiodide assay

The oxidation of I^- by vBPO produces IOH, which spontaneously reacts according to reaction 1 (Fig. 1) to form molecular iodine (I_2) [18]. At high I^- concentrations, the complexation of I_2 and I^- is possible and I_3^- is formed according to reaction 2. The determination of iodoperoxidase activity by the triiodide assay is based on the detection of I_3^- at 350 nm ($\varepsilon = 25\ mM^{-1}\ cm^{-1}$). However, I_3^- is a secondary product of the enzymatic reaction, and accurate I_2 titration is conditioned by the strength of I^-/I_2 complexation. In this context, it is necessary to have a clear understanding of the relations among pH, I^-, I_2, and I_3^- concentrations in solution.

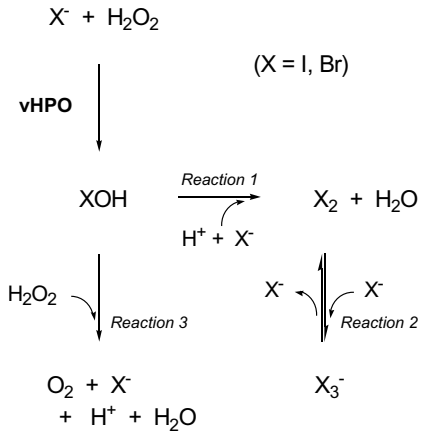

Fig. 1. Reactions involved in the vHPO-catalyzed oxidation of iodide and bromide.

The I_3^- complex formed by I_2 and I^- association is weak, as illustrated by a poor equilibrium constant ($K_{eq} = 830\ M^{-1}$ [18]). It is possible to calculate from this parameter the domain of I^- concentration for which I_3^- truly represents the I_2 concentration (i.e., I_2 is associated mainly with I^-). The iodine species concentrations can be determined using the following equations:

$$K_{eq} = [I_3^-]/([I_2][I^-]) \quad (1)$$

$$[I_2] = [I_2]_0 - [I_3^-] \quad (2)$$

$$[I^-] = [I^-]_0 - [I_3^-], \quad (3)$$

where $[I_2]_0$ and $[I^-]_0$ represent initial concentrations and $[I_2]$, $[I^-]$, and $[I_3^-]$ represent the actual concentrations. Eqs. (1)–(3) can be transformed to

$$[I^-]_0 = a[I_2]_0 + a/(K_{eq} - a(K_{eq})), \quad (4)$$

where $a = [I_3^-]/[I_2]_0$. The representation of $[I_3^-]/[I_2]_0$ as a function of $[I_2]_0$ and $[I^-]_0$ (Fig. 2) shows that triiodide is quantitatively formed (i.e., by > 95%) only when either $[I^-]$ or $[I_2]$ is more than 20 mM in the reaction mixture. In consequence, I^- is used at high concentrations in the triiodide assay to "see" I_2 formation. This was pointed out previously in a study on the lactoperoxidase/H_2O_2/X^- catalytic system [19]. The requirement of high iodide concentrations is a major drawback because the kinetic parameters of iodide for vHPOs (i.e., K_m^I) will be artificially "stacked" in the low millimolar range. The K_m^I values of various native vHPOs were determined using the triiodide assay and were reported to lie consistently in the range of 1 to 5 mM [15,16,20].

Another important limitation is due to the IOH-assisted oxidation of H_2O_2 (Fig. 1, reaction 3), which is known to be important in alkaline solutions [21]. To estimate the extent of this reaction in conditions close to those of the triiodide assay, we measured the velocities of I_3^- degradation in mixed I^- (10 mM), I_2 (0.5 mM), and H_2O_2 (2 mM) as a function of pH. We found that

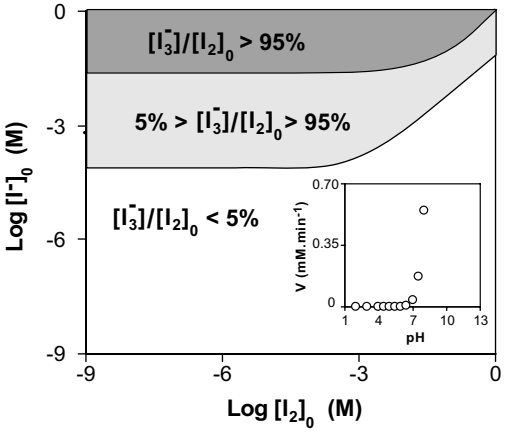

Fig. 2. Domains of I_3^- stability. The main diagram represents the domains of $[I_3^-]/[I_2]_0$ as a function of $[I_2]_0$ and $[I^-]_0$ in an aqueous solution. I_3^- concentrations were calculated from the equilibrium constant ($K_{eq} = 830\ M^{-1}$) of reaction 2 (see Fig. 1) for a range of 10^{-9} to 1 M $[I_2]_0$ and $[I^-]_0$. The domains for which $[I_3^-]/[I_2]_0$ is 0 to 5%, 5 to 95%, and 95 to 100% are represented. The inset shows the reaction rates of I_3^- degradation in H_2O_2 (2 mM), I_2 (0.5 mM), and I^- (10 mM) in acetate/borate phosphate buffers at 20 ± 1 °C. Absorbance at 350 nm was recorded, and initial velocities (0–2 min) were reported as a function of pH. Shown are the mean values of triplicates (SD < 8%).

I_3^- was unstable for pH > 6.5 (Fig. 2, inset), showing that the triiodide assay is limited to the measurement of iodoperoxidase activities in acidic solutions only. Taken together, these features clearly indicate that vHPO activities determined by the triiodide assay are controlled by the chemistry of iodine in solution rather than enzyme activity. In consequence, we believe that the I_3^- assay should be used only for qualitative applications.

Identification of TB as a probe for HPO activity

We preliminarily tested several organic dye molecules for their ability to induce significant spectral modifications in vHPO/H_2O_2/I^- and vHPO/H_2O_2/Br^- catalytic systems. We found that TB was the most effective probe in both cases. In the presence of halide (1.5 mM I^- or 10 mM Br^-), hydrogen peroxide (0.35 mM), and TB (100 μM), the vHPO-catalyzed reactions were accompanied by a large shift in the spectral properties of the solutions. At pH 8.0, the reaction media turned from yellow (λ_{max} = 430 nm) to deep blue (λ_{max} = 620 nm). The reactions between TB and vHPO/H_2O_2/X^- (X^- = I^-, Br^-) in phosphate buffer (100 mM, pH 8.0) were examined at different times during the course of the reaction using HPLC–MS. The results showed that TBI_2, on the one hand, and $TBBr_2$, on the other, were gradually and quantitatively formed with respect to TB. The rates of TBI_2 and $TBBr_2$ formation were proportional to the increase of A_{620} in the reaction mixture. In the case of iodide, triiodide accumulation (350 nm) was not observed. In the case of bromide, when MCD was added to the reaction mixture, the rate of $TBBr_2$ formation was halved, showing that the reactivity of TB toward the brominating species was equivalent to that of MCD. In both cases, the A_{620} values as a function of time were linear throughout the time course of the reactions (Fig. 3). Taken together, these results indicate that X^+ (=XOH, X_2) species are trapped by the sulfonphthalein dye before being degraded by the H_2O_2 oxidation reaction (Fig. 1, reaction 3). Thus, the rates of TB halogenation by X^+ species might not be considered as limiting in the overall reaction sequence. This observation is in agreement with the high reactivity of two-electron oxidized iodine species toward activated phenol derivatives. During the time of measurement, TB did not react in the absence of enzyme in both cases (Fig. 3), showing that the noncatalytic reaction between TB and H_2O_2/X^- is much slower than the enzyme-catalyzed reaction. In the case of iodide, the A_{620} was steady after the reaction completion, showing that TBI_2 is stable in the assay conditions. In the case of bromide and when high concentrations of H_2O_2 were used (> 0.5 mM), we observed a decrease in A_{620} after completion of the reaction, indicating a degradation of $TBBr_2$ by unknown mechanisms. Nevertheless, this side reaction is absent at initial times and, thus, can be ignored when the initial velocities are measured. Finally, we measured the relationship between vHPO concentration and initial rates of A_{620} modifications in both systems. We found that the reaction velocity is directly proportional to enzyme concentration in a range from 0.05 to 4.0 μg ml^{-1} (Fig. 3, insets).

To demonstrate the direct involvement of TBI_2 and $TBBr_2$ in the increase in A_{620}, and to better understand the relation between enzymatic activity and spectral modification at a molecular level, we conducted enzymatic reactions on a preparative scale to isolate the respective products. TBI_2 was isolated after acidification of the reaction mixture and dichloromethane extraction. The resulting TBI_2 (90% yield) was pure at > 99% (HPLC–MS). The exact mass determination by HRMS confirmed the elemental composition of TBI_2 (calculated for $C_{27}H_{27}I_2O_5S$: 716.9669, found 716.9639). $TBBr_2$ was isolated using the same procedure and was further purified using preparative thin-layer chromatography. The resulting $TBBr_2$ (28% yield) was pure at > 99% (HPLC–MS). The exact mass determination by HRMS confirmed the elemental composition of $TBBr_2$ (calculated for $C_{27}H_{27}$[79]Br[81]BrO_5S: 622.9925, found 622.9902).

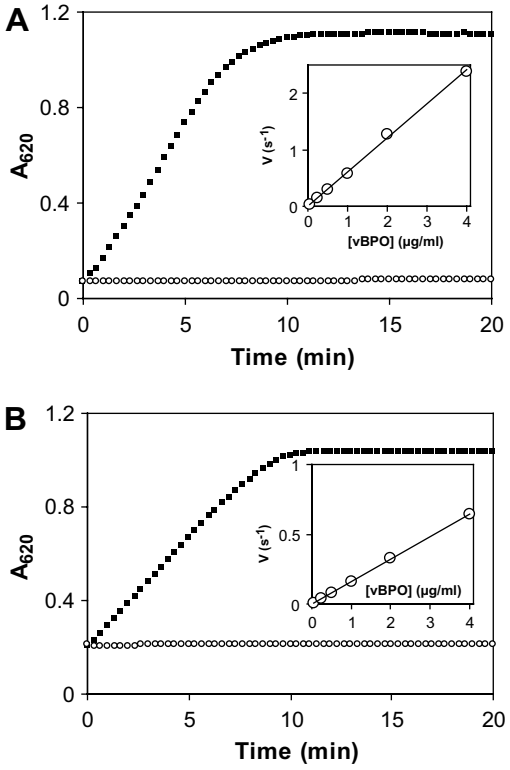

Fig. 3. Time-dependent vBPO-catalyzed oxidation of bromide and iodide. (A) TB (100 μM), NaI (1.5 mM), vBPO (■, 0.25 μg ml^{-1}; ○, no enzyme), and H_2O_2 (0.35 mM) were mixed in phosphate buffer (100 mM, pH 8.0) at 20 ± 1 °C, and the absorbance at 620 nm was immediately recorded during 20 min. In the inset, the initial velocities of A_{620} increase (0–60 s) are reported as a function of [vBPO] (0.05–4.0 μg ml^{-1}). (B) TB (100 μM), NaBr (10 mM), vBPO (■, 0.6 μg ml^{-1}; ○, no enzyme), and H_2O_2 (0.1 mM) were mixed in phosphate buffer (100 mM, pH 8.0), and the absorbance at 620 nm was immediately recorded during 20 min. In the inset, the initial velocities of A_{620} increase (0–60 s) are reported as a function of [vBPO] (0.05–4.0 μg ml^{-1}). Shown are the mean values of quadruplicates. For reasons of clarity, standard deviations (<6%) are not shown.

The neat compounds were dissolved in phosphate buffer (100 mM, pH 8.0), and the spectral properties of these solutions were found to be identical to those of the previously described mixture of vHPO, H_2O_2, KX (X = I, Br), and TB after the completion of the reaction. This result confirmed that TBI_2 and $TBBr_2$ are responsible for the absorbance at 620 nm. At pH 8.0, the molar extinction coefficient of TBI_2 at 620 nm (ε^{620}) was 40,300 M^{-1} cm^{-1}, that of $TBBr_2$ was 37,200 M^{-1} cm^{-1}, and that of TB was 2500 M^{-1} cm^{-1}. The pK_a of TBI_2 was 7.3, that of $TBBr_2$ was 7.2, and that of TB was 8.9. Therefore, the color shift observed in our assay is explained by the large pK_a shift on halogenation of the sulfonphthalein dye. In the assay conditions, the pK_a of TB (8.9) is higher than the pH (8.0). Thus, the yellow form of TB is represented by formula **1,** which is a monoanionic compound containing a quinoid group (Fig. 4A) [22]. Compound **1** absorbs energy in the violet region of the spectrum; therefore, the color transmitted by its solutions is yellow (Fig. 4B). The halogenation of TB produces a new compound with a pK_a (7.3 or 7.2 for TBI_2 or $TBBr_2$, respectively) that is lower than the pH (8.0). As a consequence, the dihalosulfonphthalein is deprotonated and stabilizes in a dianionic quinone–phenolate form represented by formula **2** responsible for the deep blue color (Fig. 4B) [23]. In this category of reaction, the electrophilic substitution by X^+ species always takes place at ortho positions of electron-donating substituents. It is important to note that the assay is inherently restricted to a narrow range of running pH, corresponding to a domain between the pK_a of TB and that of

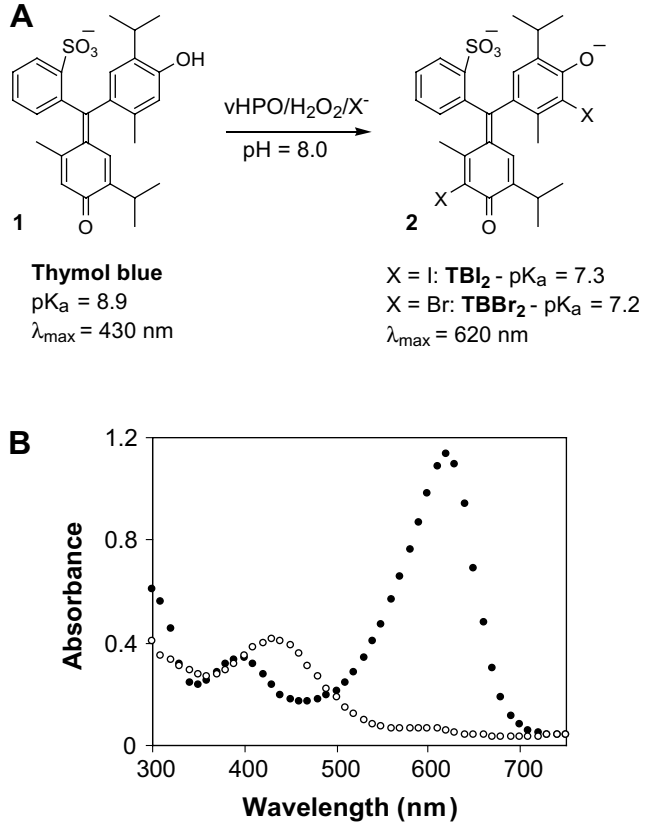

Fig. 4. Reaction of TB toward the vBPO-catalyzed oxidation of iodide and bromide. (A) At pH 8.0, TB (pK_a = 8.9) is represented by the monoanionic quinoid formula **1**, responsible for the yellow color (λ_{max} = 430 nm). The vBPO-catalyzed halogenation of TB produces TBI_2 (pK_a = 7.3) or $TBBr_2$ (pK_a = 7.2). Subsequent deprotonation results in the dianionic quinone–phenolate form **2,** responsible for the deep blue color (λ_{max} = 620 nm). (B) Absorbance of TB (○) and TBI_2 (●) in phosphate buffer (100 mM, pH 8.0) and 2% DMSO recorded between 300 and 750 nm. The UV–visible spectrum of $TBBr_2$ was similar to that of TBI_2 and is not shown.

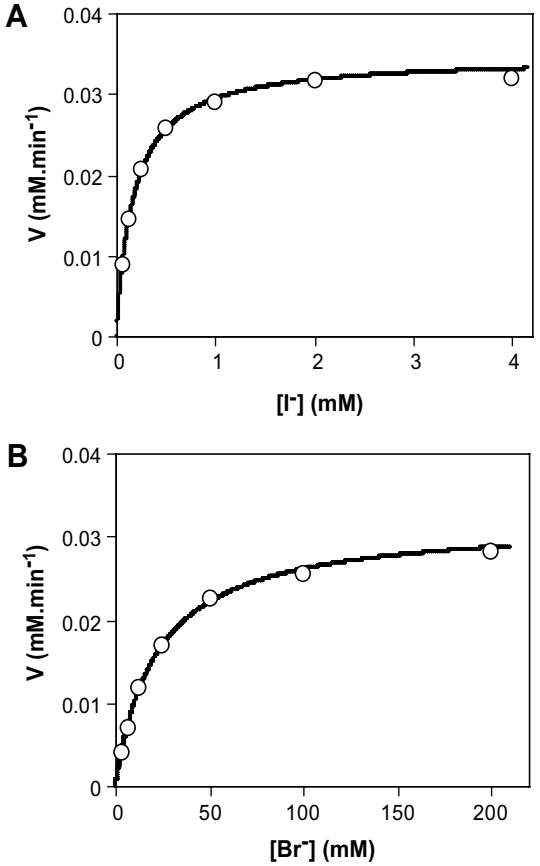

Fig. 5. Determination of K_m and k_{cat} values of iodide and bromide for vanadium bromoperoxidase from *A. nodosum*. The assays were performed at 20 ± 1 °C in a 96-well microplate. TB (100 μM), NaI (62.5 μM–4 mM) (A) or NaBr (3.125–200 mM) (B), vBPO (0.5 μg ml^{-1}), and H_2O_2 (0.2 mM) were mixed in phosphate buffer (100 mM, pH 8,0), and the absorbance at 620 nm was immediately recorded. The kinetic parameters K_m and V_{max} were calculated by fitting the experimental data to the Michaelis–Menten equation using a nonlinear regression program developed in Visual Basic for Excel. k_{cat} values were obtained from $k_{cat} = V_{max}/E_t$, where E_t is the total concentration of vBPO regarding the monomer (MW = 65,000 g mol^{-1}). Shown are the mean values of quadruplicates. For reasons of clarity, standard deviations (<8%) are not shown.

TBI_2 or $TBBr_2$. Typically, a buffered solution of pH 8.0 should be used.

Kinetic parameters of vBPO from A. nodosum

We measured the initial velocities of TB halogenation as a function of I^- and Br^- concentrations in the presence of vBPO from *A. nodosum*. The concentrations of H_2O_2 were fixed at 0.2 mM to ensure enzyme saturation (K_m of H_2O_2 = 22 μM at pH 7.92 [9]). We found that, in both cases, the relation corresponds to that of a rectangular hyperbola (Fig. 5). At low [X^-], the rate of the reaction increases proportionally to substrate concentration. At higher [X^-], the rate of the reaction remains constant, indicating a saturation of enzyme activity. The nonlinear fit of the initial velocities versus [I^-] resulted in a K_m^I of 0.18 mM and a k_{cat} of 75 s^{-1}. The curve fit of the initial velocities versus [Br^-] resulted in a K_m^{Br} of 22 mM and a k_{cat} of 71 s^{-1}. These results are not significantly different from reported values calculated using the initial velocities of MCD bromination (K_m^{Br} = 19mM, k_{cat} of 50 s^{-1} at pH 7.92 [9]). We also determined half-saturation constants for various H_2O_2 concentrations and found consistent values (K_m^I values were 0.18, 0.22, 0.20, and 0.19 mM, and K_m^{Br} values were 22, 22, 24, and 21 mM, at 0.20, 0.35, 0.7, and 1.0 mM H_2O_2, respectively). These results demonstrate that the method described here efficiently estimates the kinetic parameters for the enzyme. The half-saturation constant of bromide was found to be consistently approximately 100-fold larger than that of iodide. It is important to note that a mechanism by which the halide is directly and irreversibly engaged in the catalytic cycle has been assumed for vBPOs [9] and for Feheme peroxidases [24]. This mechanism is reinforced by the fact that the existence of a halide binding pocket and/or reversible halide fixation has never been demonstrated. In this context, the K_m values are not a measure of binding strength ($K_m = K_d = k_{off}/k_{on}$) but rather a measure of oxidation efficiency for a given substrate ($K_m = k_{cat}/k_{on}$). Thus, estimates of bimolecular rate constants (k_{on}) can be obtained by dividing k_{cat} by K_m ($k_{on} = 4.2 \times 10^5$ and 3.2×10^3 M^{-1} s^{-1} for I^- and Br^-, respectively) [25]. On the other hand, the maximum turnover numbers were found to be identical (k_{cat} = 75 and 71 s^{-1} for I^- and Br^-, respectively), suggesting that the rate-limiting step defined as the E–OX breakdown is not influenced by the nature of the halogen. Thus, we propose that halide selectivity is driven by chemical reactivity of the peroxovanadium intermediate rather than molecular recognition in a binding pocket. This mechanism is supported by the reduction potential values of IOH/I^- ($E_{1/2}$ = 0.76 V at pH 7.8) and BrOH/Br^- ($E_{1/2}$ = 1.10 V at pH 7.8) as well as by the fact that all known vBPO can oxidize Br^- and I^- and all known vCPO can oxidize Cl^-, Br^-, and I^-. This type of selectivity is standard for a transition metal catalyst whose reactivity can be easily altered by changing the coordination sphere with appropriate ligands.

In conclusion, we have developed an accurate and sensitive colorimetric assay for the titration of haloperoxidase activities. The method is based on the specific increase in absorbance at 620 nm that occurs on the halogenation of TB. The quantitative determination of both iodo- and bromoperoxidase activities with the same assay is now possible. This method can be applied to the analysis of a large number of samples, and the wavelength of detection is far less susceptible to interference than that of the triiodide assay. This methodology opens new perspectives in studying the catalytic mechanism of halide oxidation by vanadium- and Feheme-dependent haloperoxidases.

Acknowledgment

This work was supported by the Environmental Nuclear Toxicology program and CEA–iBiTecS.

References

[1] G.W. Gribble, The diversity of naturally produced organohalogens, Chemosphere 52 (2003) 289–297.
[2] F.H. Vaillancourt, E. Yeh, D.A. Vosburg, S. Garneau-Tsodikova, C.T. Walsh, Nature's inventory of halogenation catalysts: Oxidative strategies predominate, Chem. Rev. 106 (2006) 3364–3378.
[3] L.P. Hager, D.R. Morris, F.S. Brown, H. Eberwein, Chloroperoxidase: Utilization of halogen anions, J. Biol. Chem. 241 (1966) 1769–1777.
[4] S.P. Porterfield, C.E. Heindrich, The role of thyroid hormones in prenatal and neonatal neurological development: Current perspectives, Endocr. Rev. 14 (1993) 94–106.
[5] P.G. Furtmüller, M. Zederbauer, W. Jantschko, J. Helm, M. Bogner, C. Jakopitsch, C. Obinger, Active site structure and catalytic mechanisms of human peroxidases, Arch. Biochem. Biophys. 445 (2006) 199–213.
[6] C. Leblanc, C. Colin, A. Cosse, L. Delage, S. La Barre, P. Morin, B. Fiévet, C. Voiseux, Y. Ambroise, E. Verhaeghe, D. Amouroux, O. Donard, E. Tessier, P. Potin, Iodine transfers in the coastal marine environment: The key role of brown algae and of their vanadium-dependent haloperoxidases, Biochimie 88 (2006) 1773–1785.
[7] A. Butler, J.N. Carter-Franklin, The role of vanadium bromoperoxidase in the biosynthesis of halogenated marine natural products, Nat. Prod. Rep. 21 (2004) 180–188.
[8] K.M. Manoj, Chlorinations catalyzed by chloroperoxidase occur via diffusible intermediate(s), and the reaction components play multiple roles in the overall process, Biochim. Biophys. Acta 1764 (2006) 1325–1329.
[9] E. de Boer, R. Wever, The reaction mechanism of the novel vanadium–bromoperoxidase: A steady-state kinetic analysis, J. Biol. Chem. 263 (1988) 12326–12332.
[10] D.C. Crans, J.J. Smee, E. Gaidamauskas, L. Yang, The chemistry and biochemistry of vanadium and the biological activities exerted by vanadium compounds, Chem. Rev. 104 (2004) 849–902.
[11] R.R. Everett, H.S. Soedjak, A. Butler, Mechanism of dioxygen formation catalyzed by vanadium bromoperoxidase: Steady state kinetic analysis and comparison to the mechanism of bromination, J. Biol. Chem. 265 (1990) 15671–15679.
[12] E. de Boer, H. Plat, M.G.M. Tromp, R. Wever, M.C.R. Franssen, H.C. Van der Plas, E.M. Meijer, H.E. Schoemaker, Vanadium containing bromoperoxidase: An example of an oxidoreductase with high operational stability in aqueous and organic media, Biotechnol. Bioeng. 30 (1987) 607–610.
[13] H.S. Soedjak, A. Butler, Chlorination catalyzed by vanadium bromoperoxidase, Inorg. Chem. 29 (1990) 5015–5017.
[14] H. Vilter, Vanadium-dependent haloperoxidases, in: H. Sigel, A. Sigel (Eds.), Metal Ions in Biological Systems, Marcel Dekker, New York, 1995, pp. 325–362.
[15] C. Colin, C. Leblanc, G. Michel, E. Wagner, E. Leize-Wagner, A. Van Dorsselaer, P. Potin, Vanadium-dependent iodoperoxidases in *Laminaria digitata,* a novel biochemical function diverging from brown algal bromoperoxidases, J. Biol. Inorg. Chem. 10 (2005) 156–166.
[16] M. Almeida, S. Filipe, M. Humanes, M.F. Maia, R. Melo, N. Severino, J.A.L. da Silva, J.J.R. Frausto da Silva, R. Wever, Vanadium haloperoxidases from brown algae of the Laminariaceae family, Phytochemistry 57 (2001) 633–642.
[17] H. Vilter, Extraction of proteins from sources containing tannins and anionic mucilages, Methods Enzymol. 228 (1994) 665–672.
[18] M. Eigen, K. Kustin, The kinetics of halogen hydrolysis, J. Am. Chem. Soc. 84 (1962) 1355–1361.
[19] M. Huwiler, H. Kohler, Pseudo-catalytic degradation of hydrogen peroxide in the lactoperoxidase/H_2O_2/iodide system, Eur. J. Biochem. 141 (1984) 69–74.
[20] J.N. Carter, K.E. Beatty, M.T. Simpson, A. Butler, Reactivity of recombinant and mutant vanadium bromoperoxidase from the red alga *Corallina officinalis*, J. Biol. Inorg. Chem. 91 (2002) 59–69.
[21] H.A. Liebhafsky, L.S. Wu, Reactions involving hydrogen peroxide, iodine, and iodate ion: V. Introduction to the oscillatory decomposition of hydrogen peroxide, J. Am. Chem. Soc. 96 (1974) 7180–7187.
[22] N.O. McHedlov-Petrosyan, Y.N. Surov, V.A. Trofimov, A.Y. Tsivadze, Vibrational spectra of certain triphenylmethane dyes and their structure in solution, Theor. Exp. Chem. 26 (1991) 644–653.
[23] P. Balderas-Hernández, M.T. Ramírez-Silva, M. Romero-Romo, M. Palomar-Pardavé, G. Roa-Morales, C. Barrera-Diaz, A. Rojas-Hernández, Experimental correlation between the pK_a value of sulfonphthaleins with the nature of the substituent groups, Spectrochim. Acta A 69 (2008) 1235–1245.
[24] H.B. Dunford, Peroxidases in Chemistry and Biology, CRC Press, Boca Raton, FL, 1991.
[25] V. Bloomfield, L. Peller, R.A. Alberty, Multiple intermediates in steady-state enzyme kinetics: II. Systems involving two reactants and two products, J. Am. Chem. Soc. 84 (1962) 4367–4374.